

Coulomb Excitation Process in the Lighter Odd-Mass Nuclei*

G. M. TEMMER AND N. P. HEYDENBURG

Department of Terrestrial Magnetism, Carnegie Institution of Washington, Washington, D. C.

(Received June 21, 1954)

We have studied the Coulomb excitation functions for thin targets of F^{19} , Na^{23} , Ti^{47} , Mn^{55} , and Ge^{73} , and for thick targets of V^{51} and Fe^{57} , with alpha particles up to 3.5 Mev; the energy levels excited in these nuclei are at 113 and 196 kev, 446 kev, 160 kev, 128 kev, 68 kev, 320 kev, and 137 kev, respectively. The de-excitation gamma rays from these levels to the ground states were detected except for Fe^{57} , where a 123-kev gamma ray is predominantly emitted. In addition, we have excited the 182-kev level in Zn^{67} , whose de-excitation takes place partly by cascade through the 92-kev first excited state. In the cases of F^{19} and Na^{23} we were able to compare directly the relative contributions of Coulomb excitation and compound nucleus formation by means of the $(\alpha, p\gamma)$ reactions taking place via the same compound nuclei. In all cases the excitation curves are in fair agreement with the theoretical $E2$ curves at the lower energies, but show definite deviations in the direction of too much excitation at the higher energies, pointing to some resonant compound-inelastic contribution as well as possible penetration effects not accounted for by the classical theory. The transition probabilities of all transitions are about one-tenth of those in the rare earth region.

A. INTRODUCTION

ONE of the advantages of using alpha particles for the Coulomb excitation of low-lying nuclear energy levels¹⁻⁴ which became immediately apparent was the possibility of studying elements of low atomic number; our early results with Mn^{55} ¹ encouraged us to pursue the present investigation. There are several reasons why ions heavier than protons are much better suited for the excitation of low- Z elements, and it might be useful to list them:

(a) The relation $2\eta = 2Z_1Z_2e^2/\hbar v \gg 1$, which must hold in order to justify the classical orbit calculations,^{5,6} is well satisfied to much lower values of Z_2 , since Z_1/v (projectile charge over incident velocity) is larger for a given bombarding energy; for alpha particles this amounts to a factor of 4 over protons. As an example, $2\eta = 8.00$ for 3-Mev alphas on $_{11}Na^{23}$.

(b) Because of the higher charge, the Coulomb barrier is higher and prevents appreciable interference of compound nucleus formation with the process of interest here until one goes to higher bombarding energies; we are thus allowed a range of energies over which Coulomb excitation is essentially the only mechanism contributing to the excitation of nuclear energy levels. This is important because (aside from lifetime determinations) Coulomb excitation is probably the best understood process today from which to extract nuclear transition matrix elements directly.

(c) Troublesome high-energy gamma radiation from

light targets is almost entirely absent with alpha particles, whereas protons produce appreciable capture radiation in the (p, γ) process (E_γ of the order of 7 Mev) up to $Z \sim 40$, thus making the detection of low-energy gamma rays from the deexcitation of low-lying levels difficult if not impossible.

(d) Many of the nuclei between $Z=20$ and $Z=50$ have (p, n) thresholds lying between 1 and 2 Mev⁷; neutron background and induced positron activities then complicate the problem considerably. In some cases we have found the gamma radiation from the $(p, n\gamma)$ reaction, i.e., from the first excited state of the nucleus $(A, Z+1)$ when bombarding with protons. This is an interesting approach in itself but does not concern us in the present investigation.

(e) Targets which are available only as compounds, such as oxides and chlorides, can be used without difficulty when bombarding with alpha particles for the reasons discussed under (c) and (d); furthermore, the problem of finding a suitably inert backing material for thin target studies is minimized. Nickel turned out to be satisfactory in this respect, but not for protons (see Mn^{55} below).

(f) Finally, general background gamma radiation from the electrostatic generator is many times higher with protons than it is with alpha particles, mainly for the same reasons as listed under (c) and (d) above as applied to the walls of the accelerator tube.

It is for these reasons that we have experienced great difficulties in the few instances where we have attempted to measure Coulomb excitation cross sections with protons; this turns out to be necessary in order to determine the multipolarity of the transitions involved, when making use of the method suggested by Bjerregaard and Huus.⁸ The lightest element so far where proton bombardment yielded useful results for us was rhodium ($Z=45$).

* A preliminary account of some of the results in this paper were presented at the Washington meeting of the American Physical Society [Phys. Rev. **95**, 629 (1954)].

¹ G. M. Temmer and N. P. Heydenburg, Phys. Rev. **94**, 351 (1954).

² N. P. Heydenburg and G. M. Temmer, Phys. Rev. **94**, 906 (1954).

³ G. M. Temmer and N. P. Heydenburg, Phys. Rev. **94**, 1399 (1954).

⁴ N. P. Heydenburg and G. M. Temmer, Phys. Rev. **95**, 861 (1954).

⁵ K. A. Ter-Martirosyan, J. Exptl. Theoret. Phys. (U.S.S.R.) **22**, 284 (1952).

⁶ K. Alder and A. Winther, Phys. Rev. **91**, 1578 (1953).

⁷ C. C. Trail and C. H. Johnson, Phys. Rev. **91**, 474 (1953).

⁸ J. H. Bjerregaard and T. Huus, Phys. Rev. **94**, 204 (1954).

The largest cross sections for Coulomb excitation were found in F^{19} (196 kev), Na^{23} (446 kev), Ti^{47} (160 kev), Mn^{55} (128 kev), and Ge^{73} (68 kev). For these we were able to perform thin-target experiments successfully. Large cross sections do not necessarily imply large matrix elements for the transitions involved; in fact, the latter turn out to be small compared to the 137-kev transition in Ta^{181} . The cross sections are large only for strictly kinematical reasons having to do with the Coulomb excitation mechanism and not with the intrinsic excitability of nuclei under study.

B. EXPERIMENTAL DETAILS

The main features of our experimental setup have already been described.⁹ In some cases we have used a

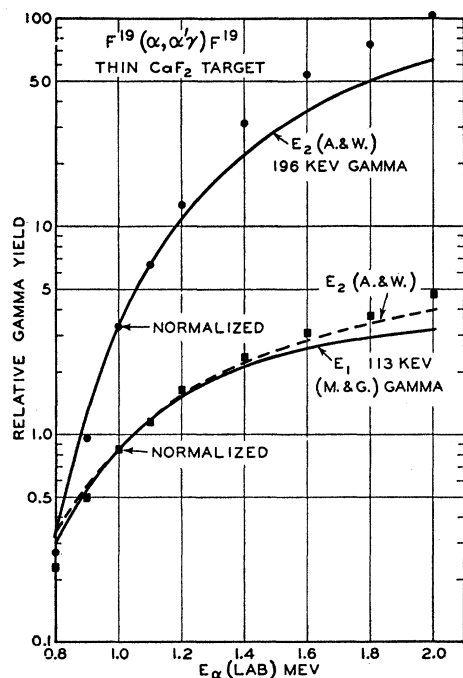


FIG. 1. Coulomb excitation by alpha particles of 113-kev and 196-kev levels in thin F^{19} target. Solid curves are theoretical E_1 (113-kev) and E_2 (196-kev) curves, according to Mullin and Guth (reference 13) and Alder and Winther (reference 6), respectively. Dashed curve is theoretical E_2 curve for comparison. Experimental points are normalized to the curves at 1 Mev. For higher-energy region, see Figs. 3 and 4 of reference 9.

Note added in proof.—Recent calculations by K. Alder and A. Winther (to be published) using the WKB approximation for the E_1 case have produced two major modifications: (a) the new definition of the parameter ξ (as discussed above); (b) the introduction of v_f (final relative velocity) in the place of v (unspecified) in their expression for the Coulomb excitation cross section (see reference 6). Modification (a) has been incorporated into this paper; modification (b) was not available in time. Suffice it to state that when this correction is applied to our results, essentially all the discrepancies between theory and experiment at the higher energies, seen in Figs. 3, 5, 6, 7, and 10, are removed. This correction is of course the larger, the greater ΔE . Only ~ 40 percent of the discrepancy disappears in the case of the 196-kev level in F^{19} .

⁹ N. P. Heydenburg and G. M. Temmer, Phys. Rev. **94**, 1252 (1954).

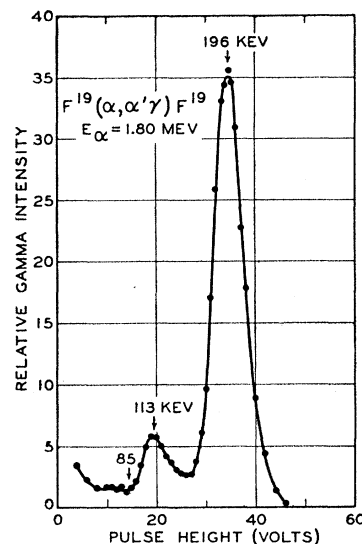


FIG. 2. Pulse-height distribution of gamma radiation from thin F^{19} target under 1.8-Mev alpha bombardment, using a well crystal. Note the absence of 83-kev cascade radiation. Note also that the peak below the 113-kev gamma ray (Fig. 5 of reference 9) has been eliminated.

2-in. \times 2-in. well-type NaI(Tl) crystal with a $\frac{3}{4}$ -in. diameter hole $1\frac{1}{2}$ in. deep, the target being located at the bottom of the well.¹⁰ In this arrangement, we approach 100-percent efficiency (including geometry) for radiations up to about 200 kev (see Fig. 1, reference 9). We were thus able to measure cross sections down to a fraction of a microbarn.

We prepared our thin targets by vacuum evaporation onto nickel backing. In the cases of Ti^{47} , Fe^{57} , Ge^{73} , and Zn^{67} we were able to obtain enriched isotopes.¹¹ We have no good measure of the target thicknesses for the thin targets, but we ascertained that they were thin enough for our purposes (~ 30 kev) by preparing targets yielding fewer gamma rays and comparing the shapes of the excitation curves. (Targets which are too thick produce characteristically steeper curves.)

C. EXCITATION FUNCTIONS

(a) F^{19}

We have previously reported some thin-target excitation functions for both the 113-kev and 196-kev levels of F^{19} under alpha-particle bombardment.⁹ In this case, we know the target to be no thicker than the width of the narrowest resonance observed in the $(\alpha, p\gamma)$ reaction (see Fig. 6, reference 9). Some additional work, extending the energy range to lower values by using our high-efficiency well crystal, is plotted in Fig. 1. These curves are in essential agreement with the work of the group

¹⁰ We are indebted to Dr. P. H. Abelson for the loan of this crystal.

¹¹ From the Oak Ridge National Laboratory, Oak Ridge, Tennessee.

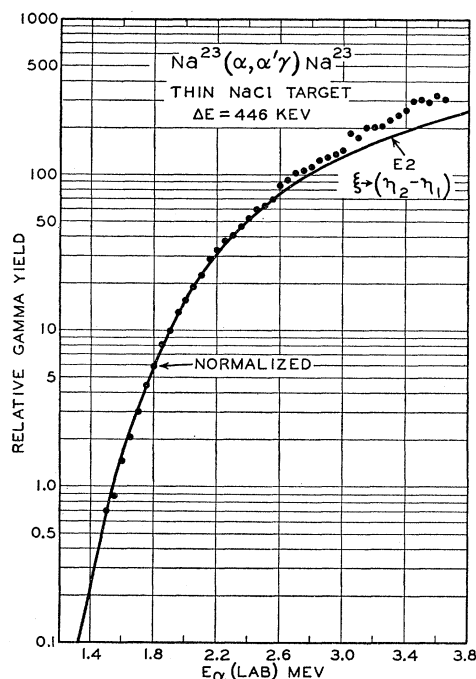


FIG. 3. Coulomb excitation function for thin NaCl target. Level energy is 446 kev. Solid curve is the theoretical $E2$ function (reference 6). Experimental points normalized at 1.8 Mev (see note added in proof, Fig. 1).

at the California Institute of Technology.¹² The theoretical curve for the electric dipole ($E1$) case is calculated according to Mullin and Guth;¹³ the curves for the electric quadrupole ($E2$) case are calculated according to the expressions given by Alder and Winther;⁶ it should be noted that the quantity $\eta_2 - \eta_1$ ($\eta_1 = Z_1 Z_2 e^2 / \hbar v_1$; $\eta_2 = Z_1 Z_2 e^2 / \hbar v_2$, v_1 and v_2 being initial and final projectile velocities, respectively) rather than

$$\xi = (\Delta E / 2E)(Z_1 Z_2 e^2 / \hbar v)$$

[which is the limiting value of $(\eta_2 - \eta_1)$ for $\Delta E/E \ll 1$, ΔE being the excitation energy, E the bombarding energy] has been used in all excitation curves, in accordance with prevailing theoretical preference. This is justified mainly by the results of the exact calculations for the electric dipole case;¹³ furthermore, the Born approximation calculation for $E2$ employing $(\eta_2 - \eta_1)$ as parameter¹⁴ seems to agree with the exact (numerical) $E2$ calculations.⁶ Incidentally, the fit with experiment is considerably improved when using the latter parameter. (Note, however, the discrepancy from theory at the higher energies.) Figure 2 shows the pulse-height distribution obtained from a thin CaF_2 target at 1.8-Mev alpha-particle energy, using the well crystal described above. Note that the satellite peak (see Fig. 5, reference 9) to the left of the 113-kev peak has disappeared. This peak seems to have also troubled Cal

¹² Sherr, Li, and Christy, Phys. Rev. **94**, 1076 (1954).

¹³ C. J. Mullin and E. Guth, Phys. Rev. **82**, 141 (1951).

¹⁴ C. J. Mullin (private communication).

Tech¹⁵ and Cavendish workers¹⁶ when studying this reaction. The absence of cascade radiation from the 196-kev level to the 113-kev level is now very evident.

(b) Na^{23}

The excitation curve for the yield of the 446-kev gamma radiation from a thin NaCl target is shown in Fig. 3. The experimental points have arbitrarily been normalized to the theoretical $E2$ curve at 1.8 Mev. The agreement over a factor of 100 in cross section is seen to be excellent, leaving little doubt as to the $E2$ nature of the excitation process.[†] The disagreement with theory at the higher energies can be attributed to some compound nucleus formation (see note added in proof, Fig. 1). With the same target we were able to obtain the excitation function for the $\text{Na}^{23}(\alpha, p\gamma)\text{Mg}^{26}$ reaction as measured by the yield of the 1.83-Mev gamma radiation resulting from the deexcitation of the first excited state of Mg^{26} (see note added in proof, Fig. 1). This

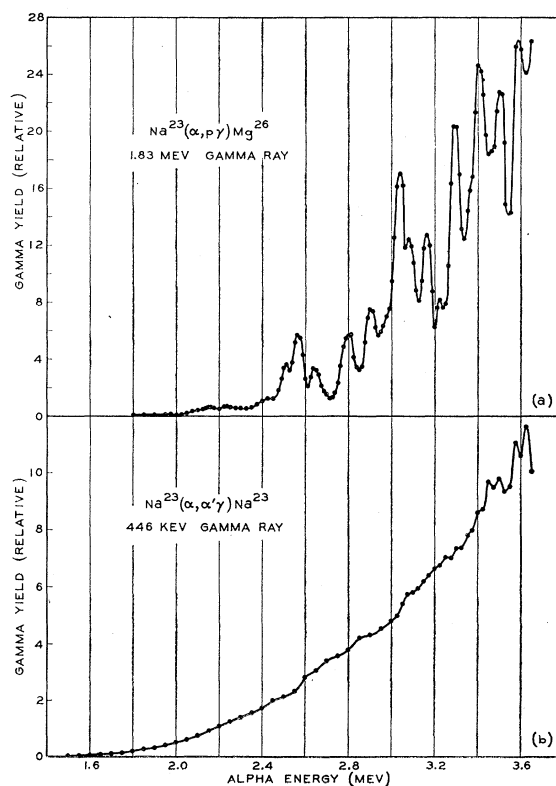


FIG. 4. (a) Excitation function for the reaction $\text{Na}^{23}(\alpha, p\gamma)\text{Mg}^{26}$, as detected by the 1.83-Mev gamma ray from Mg^{26} . Resonances are levels in the compound nucleus Al^{27} . (b) Excitation function for the reaction $\text{Na}^{23}(\alpha, \alpha'\gamma)\text{Na}^{23}$. Level energy is 446 kev. Same data as in Fig. 3. Thin NaCl target.

¹⁵ Peterson, Barnes, Fowler, and Lauritsen, Phys. Rev. **93**, 951 (1954).

¹⁶ G. A. Jones and D. H. Wilkinson, Phil. Mag. **45**, 230 (1954).

[†] Note added in proof.—The possibility that some of these transitions are of the $E1$ type cannot be completely ruled out; e.g., in the case of Na^{23} our data fall within ± 5 percent of the theoretical $E1$ curve.

reaction takes place via the compound nucleus Al^{27} . The many peaks in Fig. 4(a) correspond to levels in that nucleus, and also show that we are dealing with a thin target. In Table I we list the resonances of $Na^{23} + \alpha$ and the corresponding levels in Al^{27} . The comparison with the $Na^{23}(\alpha, \alpha'\gamma)Na^{23}$ reaction plotted in Fig. 4(b) strikingly demonstrates the interplay of Coulomb excitation and compound nucleus formation. At the high-energy end the latter excitation curve begins to show irregularities which can be correlated with levels in the compound nucleus Al^{27} as indicated in the upper curve. One can say that 3.6 Mev are about 90 percent Coulomb excitation and 10 percent compound-inelastic excitation of the 446-kev state. Also, there is undoubtedly some nonresonant excitation over and above the classically expected Coulomb excitation at the higher energies because of the gradual breakdown of the assumption $2Z_1Z_2e^2/hv \gg 1$ used in the derivation of the classical expressions.⁶

(c) Ti^{47}

The 160-kev gamma ray we reported earlier¹ was shown to belong to Ti^{47} . This gamma ray is presumably the one also seen in the beta decay of Sc^{47} .¹⁷ The thin target excitation function for an enriched target of $Ti^{47}O_2$ (82.05 percent, natural abundance 7.75 percent) is shown in Fig. 5. In this case we know that the target is no more than 50 kev thick, because we observe a resonance of about that width in the $O^{18}(\alpha, n\gamma)Ne^{21}$ reaction by means of a 342-kev gamma ray¹⁸ coming from the first excited state of Ne^{21} . The experimentally observed yields are normalized to the theoretical $E2$ curve⁶ at 2 Mev. Again, the agreement with the theory is found to be good at the lower energies, with character-

TABLE I. Levels in the compound nucleus Al^{27} as obtained from $Na^{23}(\alpha, \beta\gamma)Mg^{26}$, observing the 1.83-Mev gamma-ray yield. E_r = resonance energy in the laboratory system; $E_{c.m.}$ = resonance energy in the center-of-mass system; E^* = excitation energy of Al^{27} .

E_r (Mev)	$E_{c.m.}$ (Mev)	E^* (Mev)
1.95	1.66	12.08
2.15	1.83	12.24
2.43	1.98	12.40
2.51	2.14	12.56
2.56	2.18	13.60
2.64	2.25	12.67
2.80	2.39	12.79
2.90	2.47	12.87
3.04	2.59	13.01
3.07	2.62	13.04
3.16	2.69	13.11
3.23	2.75	13.17
3.29	2.80	13.20
3.40	2.90	13.32
3.50	2.98	13.40
3.58	3.05	13.47

¹⁷ Cork, LeBlanc, Brice, and Nester, Phys. Rev. **92**, 367 (1953).

¹⁸ This gamma ray is always present when we use oxide targets and represents the only observable effect ascribable to oxygen under alpha-particle bombardment.

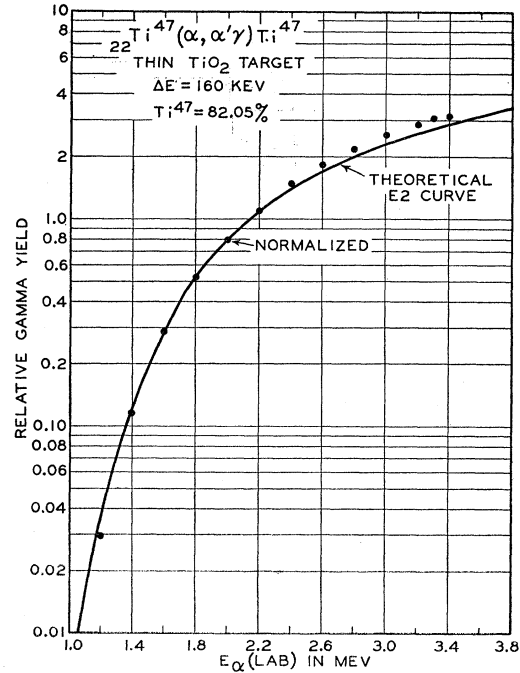


FIG. 5. Coulomb excitation function for thin enriched $Ti^{47}O_2$ target. Level energy is 160 kev. Solid curve is the theoretical $E2$ function (reference 6). Experimental points normalized at 2 Mev (see note added in proof, Fig. 1).

istic departures occurring around 2.5 Mev and above (see note added in proof, Fig. 1).

(d) Mn^{55}

We have already reported our thick-target results for the excitation of the 128-kev line from this nucleus.¹ The main reason for investigating the thin-target yield was to establish how reliable our thick-target calculations were and how much detail is generally lost when we are forced, because of intensity considerations, to confine ourselves to thick-target excitation. Figure 6 shows the thin-target curve, along with the theoretical $E2$ function.⁶ The agreement is again seen to be quite good at the lower energies, with deviations (excess over theory) becoming apparent at higher energies (see note added in proof, Fig. 1). The target used was electrolytic manganese metal evaporated on nickel foil. Generally speaking, not too much detail is lost when using thick targets, if the main objective is to measure absolute cross sections. It must be remembered that thin targets introduce the difficulty of having to know the target thickness absolutely.

In Mn^{55} we were able to make use of the comparison method⁸ already mentioned. It turns out that if the thin-target yield of the gamma radiation is measured for protons and alpha particles having the same value of the parameter ξ , the ratio of the yields will always be either 16 for $E3$, 10 for $E2$, or 6.4 for $E1$ (numerical values approximate). In the case of Mn , 1.86-Mev

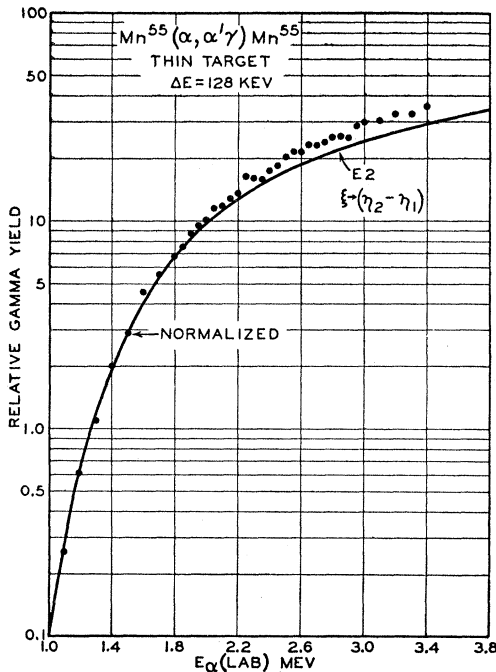


FIG. 6. Coulomb excitation function for thin Mn^{55} target. Level energy is 128 keV. Solid curve is the theoretical $E2$ function (reference 6). Experimental points normalized at 1.5 MeV. For thick-target excitation curve, see Fig. 2 of reference 1 (see note added in proof, Fig. 1).

alpha particles and 0.75-Mev protons have the same value of ξ . The experimentally observed ratio of alpha to proton yields at these energies was 10.8 ± 1.0 , thus once again confirming the $E2$ nature of the excitation process. The thin target of Mn was deposited on niobium foil, using a 0.032-in. copper absorber to reduce the Nb x-rays. Niobium was found to have a lower background than nickel for proton excitation.

(e) Fe^{57}

Even with our enriched target of Fe^{57} (59.3 percent, natural abundance 2.25 percent) in the form of Fe_2O_3 and our 4π geometry we did not have enough intensity for thin target work. The previously reported 123-keV gamma ray¹ was shown to belong to Fe^{57} as expected. The oxide was reduced at about 1000°F in a hydrogen atmosphere, the resulting iron powder was compressed into a pure Fe^{57} foil 0.002 in. thick. This step facilitated the theoretical thick-target yield calculation. The excitation curve for a thick target of pure Fe^{57} for the 123-keV gamma ray is shown in Fig. 7. The insert in Fig. 7 shows the decay scheme as recently given by Alburger and Grace.¹⁹ We are evidently exciting the second excited state of Fe^{57} at 137 keV. In order to show the sensitivity of the Coulomb excitation process to the value of the excitation energy ΔE , we have plotted the theoretical thick target yields for both $\Delta E = 123$ keV and $\Delta E = 137$

¹⁹ D. E. Alburger and M. A. Grace, Proc. Phys. Soc. A67, 280 (1954).

keV, both normalized to the experimental points at 2.0 MeV. The better agreement with the 137-keV curve is very evident. Although there is no doubt about the state of affairs in this particular instance, it is interesting to note that the excitation curve can in general decide whether a given gamma ray represents a transition to the ground state, even if the energy difference between excitation energy and gamma-ray energy were only about 10 percent.

In the gamma-ray spectrum of Fe^{57} we found evidence for gamma radiation at 14 keV, which is undoubtedly produced by cascade only, since that transition is known to be too slow ($t_{1/2} = 1.1 \times 10^{-7}$ sec) and of the wrong multipolarity ($M1$) to be Coulomb excited. We also see some slight indication for the 137-keV crossover transition, which is known to be weak compared to the 123-keV radiation (ratio of 123/137 = 15 ± 7 as found by proportional counter measurement¹⁹). Our excitation of the 137-keV level confirms the electric quadrupole nature of the transition.

We also compared the thick-target yields for Fe^{57} and $Fe_2^{57}O_3$ at 3.0 MeV in order to have some empirical information on the stopping power effect of oxygen for cases (such as the rare earths) where only oxides are available. The ratio for the yields of the 123-keV radiation was 2.07. A similar thick-target comparison for Ta and Ta_2O_5 yielded a ratio of 2.00. We shall therefore use a factor of 2 to put oxides and pure substances on a correct relative basis.

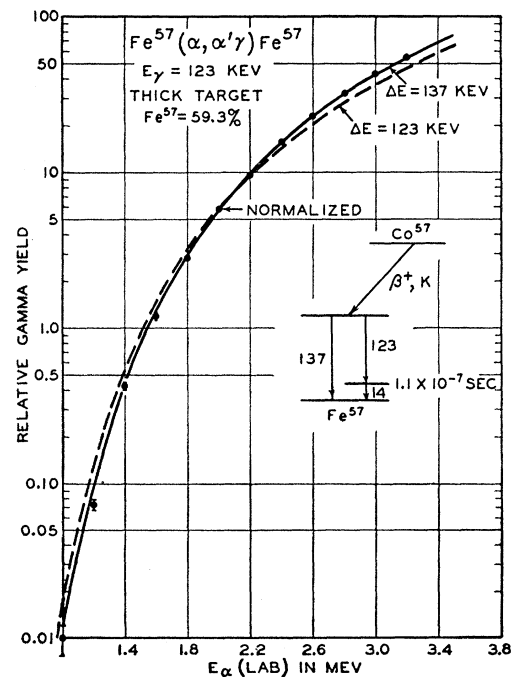


FIG. 7. Coulomb excitation function for thick enriched Fe^{57} target. Level energy is 137 keV, gamma ray detected is 123 keV. Solid curve is the theoretical $E2$ function for $\Delta E = 137$ keV, dashed curve for $\Delta E = 123$ keV. Experimental points normalized at 2 MeV. Insert shows level scheme as given in reference 19 (see note added in proof, Fig. 1).

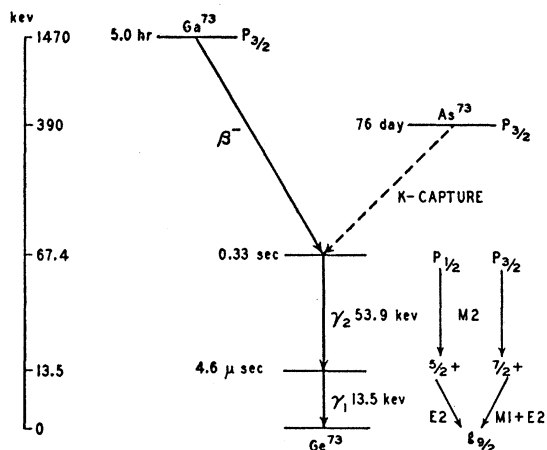


FIG. 8. Level scheme of Ge^{73} as given in reference 21. Level at 67.4 keV is not the one we excite (see text). Crossover transition to ground is less than 2×10^{-3} of the unconverted 54-keV radiation (reference 21).

(f) Ge^{72}

Our early work with ordinary GeO_2 revealed a strong gamma-ray line at 68 keV.¹ Since the only odd- A isotope of germanium is Ge^{73} , we suspected the line to belong to this isotope, since the even-even isotopes are either known or expected to have first excited states lying considerably higher (around 600 keV).²⁰ An enriched target of Ge^{73}O_2 (78.04 percent, natural abundance 7.67 percent) confirmed our expectation. Figure 8 shows the latest information given by Welker *et al.*,²¹ on the level scheme of Ge^{73} as known from the decay of Ga^{73} and As^{73} . We see that a level exists at 67.4 keV; however, the crossover gamma ray has never been seen, with an upper limit on the intensity of 2×10^{-3} compared to the unconverted 53.9-keV radiation. Furthermore, the lifetime of that level is known to be 0.33 second, which implies a Coulomb excitation cross section (if it were an $E2$ transition) about 10^{-7} times that of the 137-keV transition in tantalum. On the other hand, we were unable to detect a trace of either the 53.9-keV or the 13.5-keV radiation. Figure 9 gives the pulse-height distribution as obtained with enriched Ge^{73}O_2 . Three points locating the peak of the 67.8-keV gamma ray of ionium (Th^{230}), which is one of our calibration points, are also shown. We see that within the accuracy of our measurements the energy of the Ge^{73} line and the 68-keV ionium line is indistinguishable. We are forced to the conclusion that we are observing an energy level in Ge^{73} lying within less than 500 electron volts of a known level, but evidently having entirely different properties (spin, parity, lifetime).

Our thin-target excitation curve for this level is shown in Fig. 10. Again the agreement with the theoretical $E2$ curve⁶ is very good. This also confirms the fact

²⁰ G. Scharff-Goldhaber, *Phys. Rev.* **90**, 587 (1953).

²¹ Welker, Schardt, Friedlander, and Howland, *Phys. Rev.* **92**, 401 (1953).

that the 68-keV transition leads to the ground state (see remarks under Fe^{57}). The case of Ge^{73} points up the necessity for some caution when we try to identify gamma rays observed in Coulomb excitation with "known" gamma rays from beta- and gamma-ray spectroscopy.

D. OTHER RESULTS

(a) Zn^{67}

The pulse-height distribution of the gamma radiation from an enriched thick Zn^{67}O target (60.46 percent, natural abundance 4.11 percent) is shown in Fig. 11, along with a partial decay scheme of this nucleus as it is known from the decay of Ga^{67} ²² and Cu^{67} .²³ Two gamma rays, one at around 90 keV and one at 182 keV, were observed. Since the cascade from the 182-keV level involves a 90-keV and a 92-keV gamma ray (not resolvable by scintillation counter), it is of interest to see if the entire peak at around 90 keV can be accounted for without having to invoke direct Coulomb excitation of the first excited state. Using the best available information on internal conversion coefficients and branching ratios,²² we find that this is indeed the case. That is to say, within the accuracy of our measurements all gamma radiation originated from the Coulomb excitation of the 182-keV level in Zn^{67} . We have further confirmation of this from the observation that the intensity ratio of (90+92)-keV gamma radiation to 182-keV gamma radiation is unchanged at 6 MeV (He^{++})

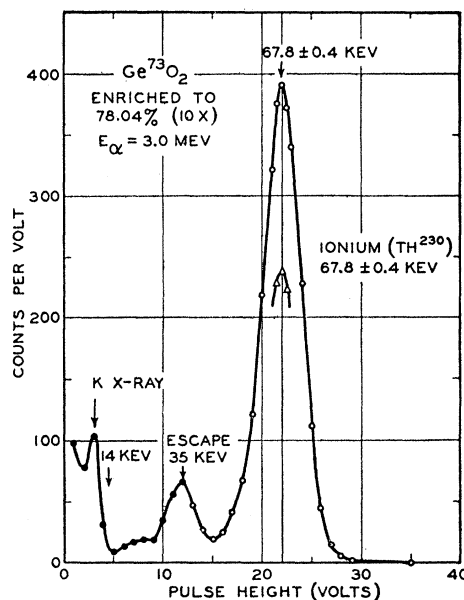


FIG. 9. Pulse-height distribution of gamma radiation from enriched Ge^{73}O_2 target, obtained with 3-Mev alpha particles. Three points under main peak locate the 67.8-keV known line from a Th^{230} calibration source. Note absence of 14-keV or 54-keV radiation.

²² Meyerhof, Mann, and West, *Phys. Rev.* **92**, 758 (1953).

²³ H. T. Easterday, *Phys. Rev.* **91**, 653 (1953).

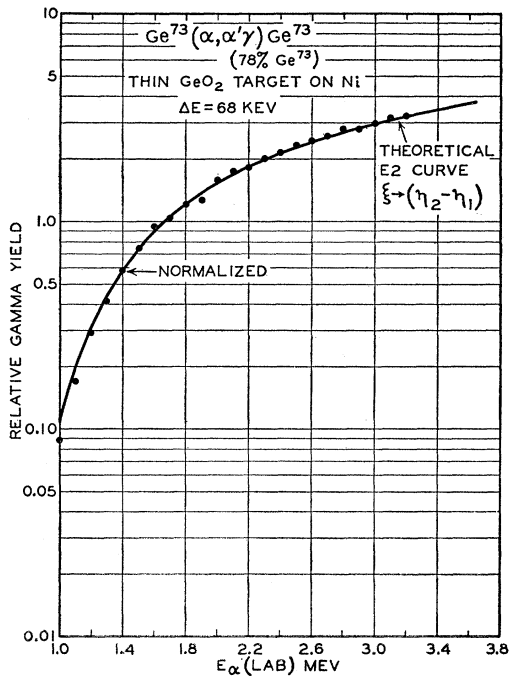


FIG. 10. Coulomb excitation function for thin enriched Ge^{73}O_2 target. Level energy is 68 kev. Solid curve is the theoretical E_2 function (reference 6). Experimental points normalized at 1.4 Mev (see note added in proof, Fig. 1).

bombarding energy; the ratio would have been altered in favor of the 182-kev line, had some direct excitation of the 92-kev level taken place. This is as it should be, since the first excited state at 92 kev is known to be isomeric with a lifetime of about 10^{-5} second; this corresponds to a very small cross section for Coulomb excitation (~ 1000 times smaller than the cross section for the 137-kev level in Ta^{181}). The spin and parity assignments which have been made for this level²² are compatible with E_2 excitation, although the return to the ground state is presumably by M_1 radiation.

(b) V^{51}

The 320-kev gamma ray associated with the first excited state of this nucleus, known from the decay of Ti^{51} ²⁴ and Cr^{51} ²⁵ as well as from inelastic proton scattering,²⁶ was observed, with an observed intensity of only about 5 percent of the other radiations discussed in this paper. We have obtained a thick-target excitation curve up to 3.4 Mev (not illustrated). Because of the relatively high location of the level, the thick-target yield varied by a factor of about 50 000 between 1.6 Mev and 3.4 Mev. The data show greater departures from the theoretical E_2 curves than the other cases described in this paper, again in a direction so as to

²⁴ Koester, Maier-Leibnitz, Mayer-Kuckuk, Schmeiser, and Schulze-Pillot, *Z. Physik* **133**, 319 (1952).

²⁵ W. S. Lyon, *Phys. Rev.* **87**, 1126 (1952).

²⁶ Hausman, Allen, Arthur, Bender, and McDole, *Phys. Rev.* **88**, 1296 (1952).

exceed the theoretical yield. Some, but not all, of this discrepancy may be ascribed to incorrectly known stopping power in this case (see note added in proof, Fig. 1).

(c) As^{75} and Se^{77}

As previously reported,¹ gamma rays of 68, 199, and 283 kev were observed in As^{75} , and of 237 and 445 kev in Se^{77} . A more detailed study of these radiations will be presented in a future publication.

We observed no other gamma radiation with 3-Mev alpha particles on nuclei with $22 < Z < 34$. We shall re-examine most of these nuclei with our 6-Mev He^{++} beam⁴ with which we should be able to excite energy levels up to about 1 Mev in the lighter nuclei, and hence several of the even-even excited states in this region.²⁷

E. CONCLUSIONS

In all cases we have studied we have verified the electric quadrupole nature of the transition involved.† We believe that on the strength of the Coulomb excitation function alone no choice can be made between the possible E_1 or E_2 character of the transition to the first excited state of F^{19} at 113 kev; in fact, the E_2 curve is seen to fit somewhat better. However, the life-

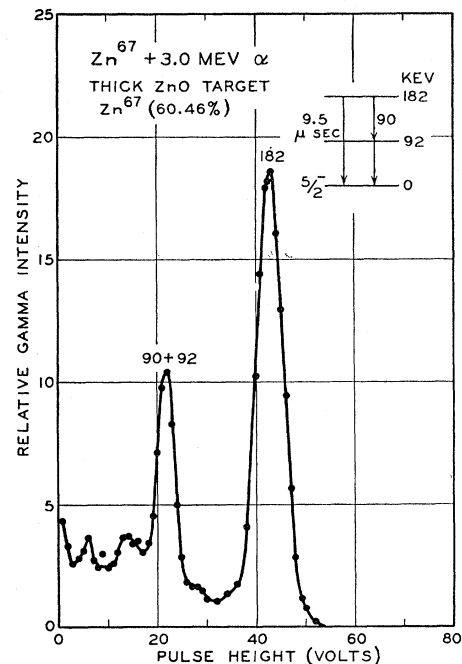


FIG. 11. Pulse-height distribution of gamma radiation from enriched Zn^{67}O target, obtained with 3-Mev alpha particles. Peak marked 90+92 is entirely accounted for by cascade transitions from the 182-kev state, without direct excitation of the 92-kev level. Partial level scheme shown as insert is taken from reference 22.

²⁷ We have already succeeded in detecting the gamma rays from the first excited states of the even-even isotopes of selenium.

time measurement²⁸ combined with the absolute value of the Coulomb excitation cross section and the isotropic angular distribution of the 113-keV radiation¹² seem to settle the question in favor of an electric dipole transition,²⁹ the only such case we have encountered among some 72 nuclei we have studied (see note added in proof, Fig. 1). Although the Coulomb excitation process favors $E1$ over $E2$ transitions by a factor of about 300 for 3-MeV alpha particles on F^{19} , the intrinsic nuclear matrix element for $E1$ is depressed about 1000-fold in this case.

Na^{23} provides a clear illustration of the interplay between Coulomb excitation and compound nucleus formation, since we have a comparison reaction proceeding via the compound nucleus Al^{27} at all energies. This case is similar to F^{19} , where we also have the $(\alpha, p\gamma)$ reaction taking place via the compound nucleus Na^{23} , as previously described.⁹

The deviations from the simple theory for $E2$ excitation evident at the high-energy end of most of these curves are presumably of two different origins: (a) compound nucleus contributions, as identified in certain favorable instances by the existence of resonances which agree with resonances of the respective compound nuclei; (b) barrier penetration effects due to the breakdown of "geometrical optics," and the existence of a finite nuclear radius (see note added in proof, Fig. 1). In view of the fact that the region of excitation in the compound nuclei involved in this investigation is completely unexplored (except for $F^{19} + \alpha$ and $Na^{23} + \alpha$) there is considerable difficulty in separating the two contributions experimentally. A more complete theory of the process can presumably hope to cope with (b) but not with (a).

In the way of spin assignments for the levels we excite, we can, of course, state that because of the $E2$ character of the transitions induced, the parities of the

TABLE II. Transition probabilities for some odd- A nuclei as found from Coulomb excitation. I_0 =ground-state spin and parity; I^* =spin of excited state (if known); ΔE =transition energy; $B_e(2)$ =reduced transition probability as defined in reference 13, obtained from thick-target yield Y_α at 3 MeV; F =ratio of observed to single-particle transition probability (using $r_0=1.2 \times 10^{-13}$ cm). Y_α is normalized to 1.00 for the 137-keV transition in Ta^{181} .

Nucleus	I_0	I^*	ΔE (keV)	$B_e(2)$ (10^{-48} cm ⁴)	Y_α	F
$^{11}Na^{23}$	3/2 ⁺	γ^+	446	0.041	1.6	71
$^{22}Ti^{47}$	5/2 ⁻	γ^-	160	0.047	4.5	31
$^{23}V^{51}$	7/2 ⁻	γ^-	320	0.013	0.41	8
$^{25}Mn^{55}$	5/2 ⁻	γ^-	128	0.070	10	38
$^{26}Fe^{57}$	(3/2 ⁻)	γ^-	137	0.051	7.5	26
$^{30}Zn^{67}$	(5/2 ⁻)	(5/2 ⁻)	182	0.043	3.7	18
$^{32}Ge^{73}$	9/2 ⁺	γ^+	68	0.042	5.8	16

excited states are equal to the respective ground-state parities, and their spins differ by 0, ± 1 , or ± 2 from the ground-state spins.

Because of the good agreement with the $E2$ theory⁶ over at least part of the energy range covered (see note added in proof, Fig. 1), we are justified in using the simple theory to estimate the relative sizes of the transition probabilities $B_e(2)$. Without making detailed corrections for variations in stopping power over the range of Z under investigation ($22 \leq Z \leq 32$; Na^{23} corrected, however) nor for internal conversion, we list in Table II the approximate transition probabilities as well as F , the ratio of observed to single-particle transition probability (using $r_0=1.2 \times 10^{-13}$ cm). We note that in all cases the transition probabilities are at least an order of magnitude smaller than the (rotational) transition in Ta^{181} (or most rare-earth nuclei). Since the latter is about 100 times what is predicted from an independent-particle model estimate, our observed values are still very much larger than is expected for single-particle transitions (with the possible exception of V^{51}). This is *a fortiori* true when compared to empirical values of transition probabilities, which usually fall short of the theoretical ones. There also seems to be no systematic difference between odd-proton and odd-neutron nuclei.

²⁸ Thirion, Barnes, and Lauritsen, Phys. Rev. **94**, 1076 (1954).

²⁹ D. H. Wilkinson (private communication) has obtained some independent evidence for the 1/2⁻ assignment for the 113-keV state from a study of the O^{19} beta decay.